Power laws in polymer solution dynamics

T. Uematsu,[1,*] C. Svanberg,[1] M. Nydén,[2] and P. Jacobsson[1]
[1]*Department of Applied Physics, Chalmers University of Technology, SE-412 96 Göteborg, Sweden*
[2]*Department of Applied Surface Chemistry, Chalmers University of Technology, SE-412 96 Göteborg, Sweden*
(Received 19 June 2003; published 24 November 2003)

The dynamical screening length ξ_h in semidilute to highly concentrated polymer solutions of poly(methyl methacrylate) in propylene carbonate has been examined using photon correlation spectroscopy and pulsed field gradient nuclear magnetic resonance. A crossover between different concentration dependent regimes, $\xi_h \sim \phi^{-\alpha}$, where α is found to be ≈ 0.5, ≈ 1, and ≈ 2, is observed when the local viscosity is taken into account. Here ϕ is the volume fraction of polymer in the solution. Well-defined crossovers between $\alpha = 0.5$ and $\alpha = 1$ corresponding to a transition from a marginal solvent to a θ solvent behavior have been predicted to occur due to the reduction of excluded-volume effects between the spatially correlated polymer segments with increasing polymer volume fraction. However, a clear experimental validation of the crossover has never been presented before. The third regime ($\alpha \approx 2$) is observed in the highly concentrated region where the static screening length is comparable to the persistence length of the polymer. The observation indicates that the rigid rod model previously used to describe concentrated solutions is an oversimplification valid only in the very high concentration limit. The obtained results at high concentrations are discussed in the frame of a simple physical model where segments at the persistence length scale are treated as flexible rodlike segments.

DOI: 10.1103/PhysRevE.68.051803 PACS number(s): 61.25.Hq, 36.20.Fz, 05.40.−a

I. INTRODUCTION

Following the seminal work by de Gennes [1] polymer solution dynamics in the dilute and the semidilute regime have been extensively studied over the past three decades. Due to the overlap of polymer chains, different concentration dependent dynamical regimes were predicted. Experimental efforts have to a large extent focused on semidilute solutions, for which the distance between the contact points, or the dynamical screening length for the hydrodynamic interaction, ξ_h, is anticipated to follow a simple power law [1,2]:

$$\xi_h \sim \phi^{-\alpha}. \tag{1}$$

Here α is 0.75, 0.5, and 1 in a good, a marginal, and a θ solvent, respectively, and ϕ is the volume fraction of the polymer. Experimentally, the validity of Eq. (1) has been examined with photon correlation spectroscopy (PCS) by probing the collective diffusion coefficient D_c, related to ξ_h via the Stokes-Einstein relation [1], i.e.,

$$D_c = \frac{k_B T}{6\pi\eta_s \xi_h}, \tag{2}$$

where k_B, T, and η_s are the Boltzmann constant, the absolute temperature, and the viscosity of the pure solvent, respectively. Thereby, a scaling prediction similar to Eq. (1) is obtained for D_c:

$$D_c \sim \phi^{\alpha}. \tag{3}$$

In the semidilute regime (typically $\phi \leqslant 0.1$) the above power laws have been confirmed for several systems [3].

Theoretical work [1,4–6] about two decades ago predicted that the exponent α would be dependent not only on the solvent quality but also on the polymer concentration. With increasing ϕ, transitions from good solvent behavior ($\alpha = 0.75$), over marginal solvent behavior ($\alpha = 0.5$), to θ solvent behavior ($\alpha = 1$) are predicted. The polymer fraction dependence originates from the commonly accepted ''thermal blob model'' [7] of polymers, which describes the distribution of the polymer sequences at different length scales. Short sequences are approximated as ideal inside a thermal blob with a radius of ξ_τ, i.e., the two-body excluded-volume effect is eliminated due to the chain stiffness [8,9]. Long sequences compared to the size of the thermal blob are fully swollen due to intramolecular interactions. Even in a good solvent, an exponent $\alpha = 0.75$ is predicted only if the two-body excluded-volume effect dominates. Thus the polymer fraction should be low (typically $\phi \leqslant 0.1$), so that ξ_τ is much lower than the static screening length for the excluded-volume interaction ξ_s. The static screening length ξ_s can be observed experimentally with, for example, x-ray and neutron scattering techniques and is assumed to be proportional to ξ_h, i.e., $\xi_h \approx 2\xi_s$, see, e.g., Ref. [3] and references therein. When the solution is concentrated further, a marginal solvent behavior ($\alpha = 0.5$) and a θ solvent behavior ($\alpha = 1$) successively take the place of the good solvent behavior due to the decrease in two-body excluded-volume effects at the ξ_s length scale. A marginal solvent behavior is predicted when the two-body excluded-volume effects become weak, i.e., when ξ_s is roughly equivalent to ξ_τ. A θ solvent behavior is predicted when the two-body excluded-volume effects vanish due to the fact that ξ_s is much smaller than ξ_τ. Furthermore, when ξ_s approaches the persistence length of the polymer, no further polymer fraction dependence ($\alpha = 0$) is predicted because a rigidlike segment is correlated over its own length. The above concepts are hereafter referred to as the ''polymer fraction dependence theory.''

*Corresponding author. Email address: uematsu@fy.chalmers.se

The polymer fraction dependence theory is experimentally very controversial. Schaefer *et al.* [2,5] have reported that a large amount of experimental data on D_c support the polymer fraction dependence theory. However, the exponents found in the marginal and the θ regimes are substantially lower than the theoretical values. Brown and Nicolai [3], on the other hand, used a common power law ($\alpha \approx 0.7$) to describe the polymer fraction dependence up to approximately $\phi = 0.3$ for well-studied polystyrene in a variety of good solvents. This result is in conflict with the polymer fraction dependence theory since, at $\phi \approx 0.3$, literature data [3,8] yield $\xi_s \approx 1$ nm and $\xi_\tau \approx 5$ nm, and thus a crossover to a θ solvent behavior should have occurred. Furthermore, in a number of studies of polymer solutions at $\phi \geqslant 0.5$, D_c is observed to decrease, thereby causing an increase in ξ_h according to Eq. (2) [10–13]. This is in sharp contrast to the $\alpha = 0$ scenario predicted by the crossover picture.

The experimental observations discussed above were all based on the assumption that the local viscosity involved in the collective diffusion is equal to the bulk viscosity of the pure solvent, η_s. However, the local viscosity is anticipated to increase with increasing polymer fraction. For example, due to the local viscosity factor, the solvent self-diffusion in polystyrene solutions observed by pulsed field gradient nuclear magnetic resonance (pfg-NMR), is significantly decreased by more than a factor of 3 at $\phi = 0.3$ [14–17]. In order to take into account the increase of the local viscosity with increasing polymer concentration, the following relations were recently proposed [18]:

$$D_c = \frac{k_B T}{6\pi \eta_{\text{local}} \xi_h}, \tag{4}$$

$$D_{sol} = \frac{k_B T}{6\pi \eta_{\text{local}} R_h^s}. \tag{5}$$

Here D_{sol}, η_{local}, and R_h^s are the self-diffusion constant of the solvent, the local viscosity, and the hydrodynamic radius of the solvent molecules, respectively. These relations are based on the assumption that the solvent molecules feel the same viscosity as the polymer segments involved in the collective diffusion. That is, the influence of topological constraints due to the entanglements of the polymer chains is neglected. The assumption is appropriate because D_c, even at this high concentration, is driven by the osmotic longitudinal elastic modulus (isothermal process) and not by the adiabatic elastic longitudinal modulus related to the topological factor [11,18].

The present paper focuses on the concentration dependence of ξ_h in solutions of poly(methyl methacrylate) (PMMA) in propylene carbonate (PC) over a large polymer concentration range. Using PCS and pfg-NMR we have been able to determine ξ_h from D_c after taking account of η_{local} using D_{sol} and Eq. (5). The present work is, to the best of our knowledge, the first investigation of polymer fraction dependence of ξ_h in PMMA solutions from the semidilute regime to the concentrated regime. PC has a high solubility in PMMA over the investigated concentration range and a low volatility with a very high boiling point (513 K). This system is thus convenient also for the study of temperature dependence of D_c and ξ_h. In this work measurements at 300 and 400 K have been performed.

II. EXPERIMENTAL DETAILS

A. Materials

In order to investigate the polymer fraction dependence of ξ_h in the semidilute and concentrated regimes the polymer solutions were prepared by mixing PC (Aldrich, high performance liquid chromatography grade) with high molecular weight PMMA (Aldrich Chemicals, $M_w = 996\,000$, $M_w/M_n = 6.97$). The composition of the samples ranges from 0 to 50 wt % PMMA. In order to check that the polydispersity of the polymer has no large influence on the collective diffusion above the dilute regime, two standard monodisperse PMMA samples ($M_w = 850\,000$, $M_w/M_n = 1.05$ and $M_w = 2\,480\,000$, $M_w/M_n = 1.16$) were also used for the polymer solutions from 1 to 5 wt % PMMA. The whole range of compositions starting from 0.5 wt % PMMA was investigated by PCS while the range 0–40 wt % PMMA was examined with pfg-NMR. To calculate the volume fraction ϕ from the weight percent of the PMMA, a semiempirical electron density calculation [19] was employed resulting in $V_{\text{PMMA}} = 155$ Å^3 and $V_{\text{PC}} = 114$ Å^3, where the PMMA volume fraction is obtained for the monomer. The samples were prepared by adding anhydrous PC to PMMA in a cylindrical sample cell. The mixture was then sealed under argon atmosphere and heated to around 400 K for 1 h to 1 day, depending on the polymer concentrations. The obtained samples were optically transparent and dust-free. The samples were finally equilibrated at room temperature for at least three months before the experiments.

B. PCS

The collective diffusion of the solutions was investigated at 300 and 400 K. The incident radiation was provided by a frequency doubled Nd-Vanadate laser (Coherent Inc.), operating at 532 nm, with vertical polarization and a typical output power of 100 mW. The scattered light was detected in homodyne fashion through a vertically oriented polarizer, digitized and fed to a correlator (ALV-5000/ FAST). The correlator covers the time range from 10^{-7} to 10^4 s and calculates the normalized autocorrelation function $g_2(q,t)$ of the scattered intensity, which is related to the structural relaxation function or the field autocorrelation function $g_1(q,t)$ by

$$g_2(q,t) = 1 + \sigma |g_1(q,t)|^2. \tag{6}$$

Here σ is the instrumental coherence factor, which in our setup is close to unity, and q is the wave vector.

C. pfg-NMR

The self-diffusion experiments were performed with a probe dedicated for diffusion measurements (DOTY Sci., USA) on a Varian Unity Inova 500 spectrometer. The echo

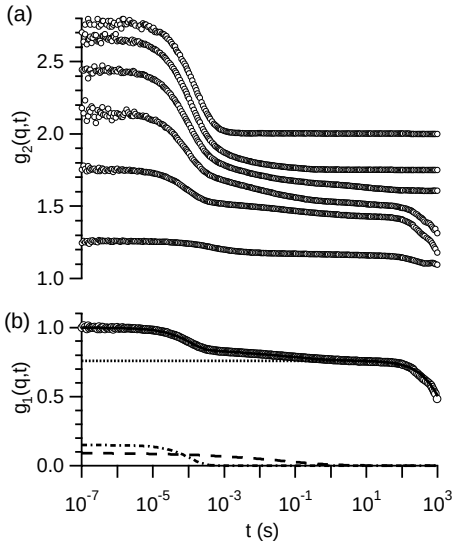

FIG. 1. Experimental data for $g_1(q,t)$ and $g_2(q,t)$ at $q=2.41\times10^{-3}/\text{Å}^{-1}$ at 300 K. (a) The lowest to the top open circles denotes $g_2(q,t)$ data for 0.5, 5, 10, 20, 30, and 50 wt % PMMA, respectively. The data are vertically shifted for clarity. (b) The open circles and the solid line represent $g_1(q,t)$ for 30 wt % PMMA and the total curve fit, respectively. The dash-dotted line, the dashed line, and the dotted line represent the fast, the intermediate, and the slow components, respectively.

decay obtained in a pfg-NMR self-diffusion experiment when performed on a monodisperse molecule as PC is expressed in terms of the normalized signal intensity I/I_0 as

$$I/I_0=\exp(-kD_{sol}). \tag{7}$$

For sine-shaped gradient pulses, $k=\gamma^2g^2\delta^2(4\Delta-\delta)/\pi^2$, where g is the gradient pulse strength, δ is the gradient pulse length, Δ is the time separation between the leading edges of the gradient pulse pair, and γ is the ^{1}H magnetogyric ratio. The gradient pulse strength was varied from 0 to maximum 0.4 T/m. Δ was 100 ms and δ was 4 ms in all experiments. The maximum gradient strength was 4.8 T/m, so that experiments were all performed in the safe limit with regards to gradient mismatch and eddy currents. The effect of temperature gradients was carefully investigated by measuring the PC self-diffusion constant D_{sol} for different Δ. If temperature gradients induced flow inside the NMR tube, this would be seen as a Δ-dependent diffusion constant. No such dependence was observed. The temperature in all experiments was 300 K.

III. RESULTS

A. Collective diffusion constants observed by PCS

In Fig. 1(a) the experimentally obtained autocorrelation function $g_2(q,t)$ for different polymer concentrations is shown, where three relaxation processes can be observed. As shown in Fig. 1(b) the corresponding field correlation function $g_1(q,t)$ is well described by

$$g_1(q,t)=\sum_{i=1}^{3}A_i\exp\left(-\frac{1}{\tau_i}\right)^{\beta_i}. \tag{8}$$

Here A_i is the amplitude of the process i, τ_i is the relaxation time, and β_i is the stretching parameter. In general, the fast process is observed as a simple exponential decay. A similar behavior is observed for the slow process although it occurs at such long time scales that it is difficult to probe with PCS. Accordingly, curve fits of Eq. (8) to experimental data are performed under the condition $\beta_1=1$ and $\beta_3=1$ in order to increase the stability of the fitting procedure.

Previous investigations of roughly identical systems have shown that the fast and slow processes are of diffusive nature [20]. This conclusion was based on the following observations: (i) single exponential decay in the intermediate scattering function, (ii) decreasing relaxation time with increasing wave vector, and (iii) an Arrhenius temperature dependence of the relaxation time. All these typical features for diffusive processes are also observed for the present system. The fast process is attributed to the so-called collective diffusion process extensively discussed in the literature [3]. This collective diffusion process has a concentration fluctuation signature, which is confirmed by the fact that the process has a significantly smaller amplitude when the polarizer is oriented horizontally. The intermediate relaxation process has previously been related to segmental mobility of the polymer matrix [20]. This conclusion was supported by the fact that this process exhibits (i) a stretched exponential for the intermediate scattering function, (ii) a non-Arrhenius temperature dependence of the average relaxation time, and (iii) no systematic wave vector dependence. We therefore attributed the intermediate process to the network dynamics characterizing the structural (longitudinal stress) relaxation of the binary solution [21,22]. In the present work the stretching parameter is in the range $0.2<\beta_2<0.4$, with the smallest values obtained for the highest concentrations. As discussed above also the slow process possesses all the features expected for diffusive dynamics. The slow process can therefore be attributed either to the reptation process of the polymer [2] or to the heterogeneity of the system [23]. This slow relaxation process is prominent in the highly concentrated regime but the amplitude decreases rapidly with decreasing polymer concentrations.

The collective diffusion constant D_c is obtained from the short scattering vector limit as

$$D_c=\frac{1}{\tau_{fast}q^2(1-\phi)}\Big|_{q\to0}, \tag{9}$$

where q is the scattering vector and $(1-\phi)$ corrects for the solvent backflow [1,2,24]. A double logarithmic plot of D_c versus ϕ at 300 and 400 K is shown in Fig. 2. Up to $\phi\approx0.02$ at 300 K, D_c is within error independent of the polymer fraction. A very weak polymer concentration dependent D_c is also expected below the number concentration, $\rho^*=3M_w(N_A4\pi R_g^3)^{-1}$, where the chains begin to overlap. Here M_w is the molecular weight and N_A is Avogadro's number. The present observation is in agreement with results for

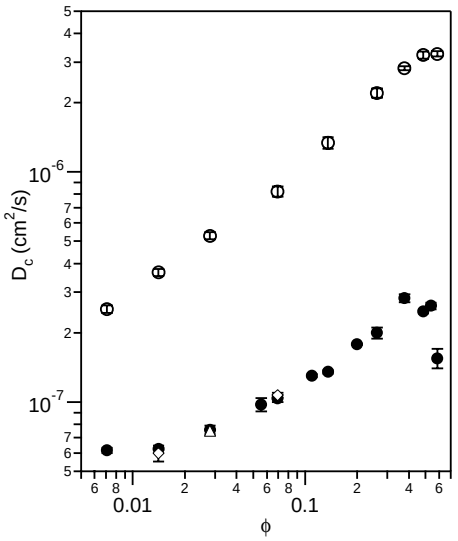

FIG. 2. Polymer volume fraction, ϕ, dependence of D_c at 300 K (the solid circles) and at 400 K (the open circles). The open triangle and open diamonds represent the data for the solutions with standard monodisperse PMMA of $M_w = 850\,000$ and $M_w = 2\,480\,000$, respectively.

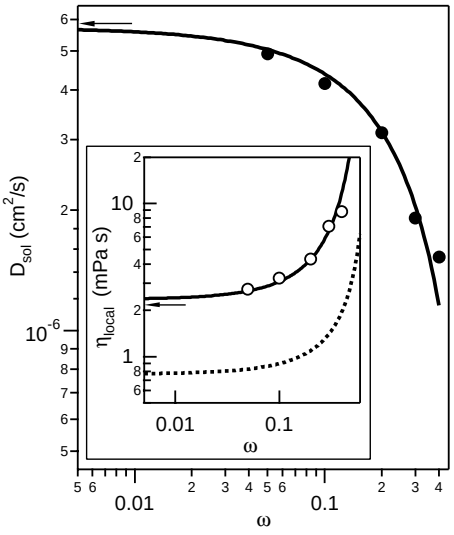

FIG. 3. Polymer weight fraction, ω, dependence of D_{sol} at 300 K. The solid circles and line represent experimental data and a free-volume theory based model proposed by Vrentas and co-workers [14–16], respectively. The inset shows the ω dependence of η_{local} at 300 and 400 K. The open circles represent the calculated data using Eq. (5). The solid line and the dotted line represent the free-volume theory at 300 and 400 K, respectively. The arrows in the main and inset figures show data at $\omega = 0$.

D_c in other dilute PMMA solutions reported recently [22,25]. From this fraction the average gyration radius R_g can be obtained: R_g (300 K) $\approx$30 nm. However, at 400 K a very weak polymer concentration dependence D_c could not be observed, indicating a larger R_g than the one at 300 K, i.e., R_g (400 K)$\geqslant$40 nm. This is probably a result of a larger excluded volume effect. When ϕ is increased further, D_c increases monotonously until the highly concentrated regime ($\phi \approx 0.4$). Above this concentration, the rate of increase in D_c at 400 K is observed to slow down considerably while a substantial drop is observed at 300 K. This latter phenomenon is well known from studies of polystyrene solutions [10–13] as mentioned in the Introduction. The results for solutions with standard monodisperse PMMA were found to be within errors identical to the results obtained with polydisperse PMMA. Thus, the polydispersity of the polymer sample does not have any significant influence on the cooperative dynamics in our investigated concentration regime.

B. Solvent self-diffusion constants observed by pfg-NMR

The solvent self-diffusion constant D_{sol} at 300 K is shown in Fig. 3. It is found that D_{sol} decreases significantly from the dilute regime in the same way as observed for other polymer solutions [14–16]. From the bulk value [26] for the viscosity of PC, $\eta_s = 2.25$ mPa s at 300 K, via Eq. (5), we obtained a hydrodynamic radius of the solvent molecules, $R_h^s = 0.16$ nm at 300 K, which is approximately equal to the rotation radius of the solvent molecule [27]. By assuming that R_h^s is independent of the polymer concentration [18], the polymer fraction dependence of η_{local} at 300 K is obtained using Eq. (5) as shown in Fig. 3. It is apparent that η_{local} at 300 K has a strong polymer concentration dependence. Thus a correction, taking the local solvent viscosity into account, significantly influences the calculation of the dynamical screening length.

In order to take η_{local} into account also in the analysis of D_c at 400 K, the D_{sol} results from 300 K can be extended by a free-volume theory based model proposed by Vrentas and co-workers [14–16]. For polymer concentrations less than about 50 wt %, the concentration and temperature dependence of D_{sol} is given [14,15] by

$$D_{sol} = D_{sol}^0 \exp\left(- \frac{\omega \psi V_p^{jump}}{(1-\omega) K_s (T - T_{0s})} \right), \qquad (10)$$

where D_{sol}^0 is a pure solvent self-diffusion constant, ω is the weight fraction of the polymer, and ψ is the ratio of the volume of the solvent molecule to the polymer jumping unit. V_p^{jump} is the specific molecular volume for the polymer jumping unit, K_s is a free-volume parameter related to the thermal expansion coefficient of the solvent, and T_{0s} is the temperature where the hole free volume of the solvent becomes zero. V_p^{jump} ($= 0.933$ cm^3/g) can be obtained from the monomer volume [19] $V_{\mathrm{PMMA}} = 155$ Å^3.

From the temperature dependence of D_{sol}^0, K_s and T_{0s} can be obtained using the free-volume theory [14,15]:

$$D_{sol}^0 = D_0 \exp\left(- \frac{V_{sol}^{jump}}{K_s (T - T_{0s})} \right). \qquad (11)$$

Here D_0 is a preexponential factor and V_{sol}^{jump} is the specific molecular volume for the solvent molecule (0.673 cm^3/g), which can be obtained from the solvent molecular volume [19] $V_{\mathrm{PC}} = 114$ Å^3. D_{sol}^0 data can be obtained from literature

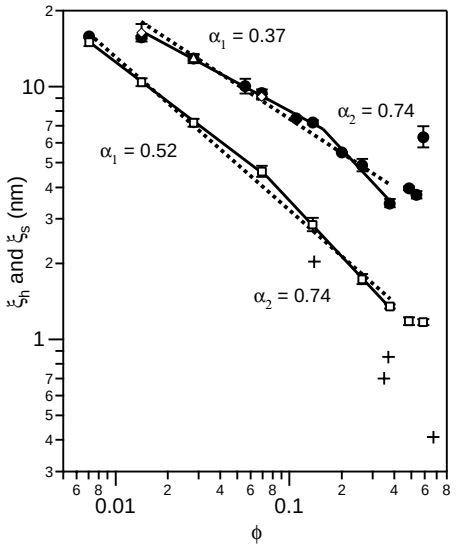

FIG. 4. Polymer volume fraction, ϕ, dependence of ξ_h at 300 K (the filled circles) and 400 K (the open squares) obtained using bulk viscosity data. The solid lines and α values represent least-squares fits and the obtained exponent in each regime. Also included for comparison are literature data for ξ_s (the crosses) at room temperature [30]. The dotted lines represent fits to single power laws; $\alpha = 0.45$ and $\alpha = 0.61$ at 300 and 400 K, respectively. The open triangle and open diamonds denote results for monodisperse PMMA.

data [26] of the solvent viscosity η_s through the relation [16] $D_{sol}^0 = C_0 T/\eta_s$, where C_0 is a constant. K_s and T_{0s} were obtained from a least-squares fit of Eq. (11) to the D_{sol}^0 data, yielding $K_s = (1.26 \pm 0.04) \times 10^{-3}$ cm^3/(g K) and $T_{0s} = 145.9 \pm 0.7$ K.

The remaining unknown parameter ψ in Eq. (10) was obtained from a least-squares fit of Eq. (10) to D_{sol} at 300 K, yielding $\psi = 0.50 \pm 0.05$. By substituting these three values in Eq. (10), the concentration dependence of D_{sol} at 400 K was obtained. Finally, η_{local} at 400 K was determined through Eq. (5) using the same assumption at 300 K, as shown in the inset of Fig. 3. The bulk value for the viscosity of PC at 400 K, $\eta_s = 0.77$ mPa s used in Eq. (5) were obtained from an extrapolation using extended free-volume theory [28,29] with literature data [26].

IV. DISCUSSION

A. ξ_h obtained using bulk viscosity data

In Fig. 4 ξ_h data obtained from D_c neglecting local viscosity effects are shown. The solvent viscosity data [26] used in Eq. (2) are $\eta_s = 2.25$ mPa s and $\eta_s = 0.77$ mPa s corresponding to 300 and 400 K, respectively. η_s at 400 K is extrapolated using the extended free-volume theory [28,29] with literature viscosity data [26].

At 300 K above $\phi \approx 0.02$ and at 400 K, two power law regimes, $\xi_h \sim \phi^{-\alpha}$, are observed. The exponents α_1 and α_2 in the regimes were obtained from a least-squares fit including four free parameters using

$$\xi_h = \begin{cases} \xi_0 \phi^{-\alpha_1}, & \phi \leqslant \phi_1 \\ \xi_0 \phi_1^{-\alpha_1+\alpha_2} \phi^{-\alpha_2}, & \phi > \phi_1, \end{cases} \tag{12}$$

where ξ_0 is a constant and ϕ_1 is the polymer volume fraction where the crossover occurs. At 300 K α_1 is found to be 0.37 for $0.02 < \phi < 0.16$ and α_2 is found to be 0.74 for $0.16 < \phi < 0.37$, respectively. At 400 K, $\alpha_1 = 0.52$ for $0.007 < \phi < 0.07$ and $\alpha_2 = 0.74$ for $0.07 < \phi < 0.37$. Thus, in the low concentration regime α_2 is found to be roughly close to the theoretical prediction for a marginal solvent ($\alpha = 0.5$) while at higher concentrations an apparent accordance with the theoretical value for a good solvent ($\alpha = 0.75$) is observed. However, the physical interpretation of this observation is indeed difficult because the expected crossover [2,5] is rather a transition from a good solvent over a marginal solvent into a θ solvent behavior with increasing ϕ. Furthermore, in Fig. 4, a good solvent behavior is observed up to $\phi = 0.37$ although it is clear that already at $\phi = 0.3$ ξ_s has approached the persistence length of PMMA [31] (≈ 1 nm) using the empirical relation [3] $\xi_h/2 \approx \xi_s$. This latter observation is also corroborated by the literature data [30] of ξ_s included in Fig. 4. The results for ξ_h are thus in clear conflict with the thermal blob model discussed in the introduction since a crossover to a θ solvent behavior ($\alpha = 1$) should have occurred below $\phi = 0.3$ according to this model.

Following instead the idea of Brown and Nicolai [3], the present data can be fitted qualitatively with a common power law ($\alpha = 0.45$ and $\alpha = 0.61$ at 300 and 400 K, respectively) up to $\phi = 0.37$ as shown in Fig. 4. However, this interpretation is obviously also in conflict with the thermal blob model. Finally, at 300 K in the highly concentrated regime ($\phi > 0.37$), ξ_h increases dramatically as shown in Fig. 4, a result that also is in conflict both with the predicted behavior and with the literature data for ξ_s obtained at room temperature [30].

B. ξ_h obtained using local viscosity data

In Fig. 5, data for ξ_h as a function of polymer concentration at 300 K and 400 K, obtained via Eq. (4), taking the local viscosity into account, are shown. In the semidilute regime ξ_h is now monotonously decreasing with ϕ as expected. A closer inspection yields a crossover at intermediate concentrations between two power law regimes with exponents roughly equal to 0.5 and 1. This is in excellent agreement with the polymer fraction dependence theory discussed in the Introduction. However, at high concentrations we observe yet another power law regime with an exponent $\alpha_3 \approx 2$, which will be further discussed below. We therefore employ a version of the extended polymer fraction dependence theory to describe our data:

$$\xi_h = \begin{cases} \xi_0 \phi^{-0.5}, & \phi \leqslant \phi_1 \\ \xi_0 \phi_1^{0.5} \phi^{-1}, & \phi_1 < \phi \leqslant \phi_2 \\ \xi_0 \phi_1^{0.5} \phi_2 \phi^{-2}, & \phi_2 < \phi. \end{cases} \tag{13}$$

Here the only free parameters are the amplitude ξ_0 and crossover polymer fractions ϕ_1 and ϕ_2. This yields an excellent

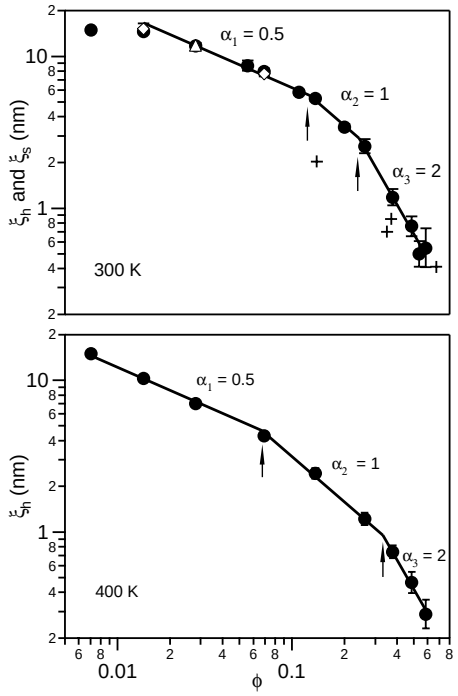

FIG. 5. Polymer volume fraction, ϕ, dependence of ξ_h at 300 and 400 K (the open squares) obtained using local viscosity data. The solid lines and α values represent least-squares fit lines and the exponent in each regime. For comparison, also included are literature data [30] for ξ_s (the crosses) at room temperature. The open triangle and open diamonds denote results for monodisperse PMMA.

description of our data as seen in Fig. 5. Furthermore, we performed complementary curve fitting with also the three exponents as free parameters. Such a curve-fit procedure yields the exponents that are, within the experimental uncertainty, equal to 0.5, 1, and 2, respectively. It is also reassuring to the note that this curve-fit procedure does not change ϕ_1 and ϕ_2 significantly. As shown in Fig. 5 a crossover from a marginal solvent behavior ($\alpha_1=0.5$) to a θ solvent behavior ($\alpha_2=1$) occurs at an intermediate concentration $\phi^\dagger \approx 0.1$ for both temperatures. However, no transition between a good solvent behavior and marginal solvent is observed at lower fractions. A good solvent behavior is, in fact, only expected in to be seen in high molecular weight polymer systems where the overlap concentration ρ^* is lower than in the present system.

More notably, in the highly concentrated regime a crossover to a new power law dependence ($\alpha_3 \approx 2$) is found. This behavior is not predicted by the polymer fraction dependence theory. However, exponents close to 2 have been observed previously for ξ_s at around $\phi=0.3$ for polystyrene in toluene [32] and for poly(dimethylsiloxane) (PDMS), in octane [33]. In support of the present findings at high concentrations are also the literature data [30] of the concentration dependence of ξ_s (included in Fig. 5 observed by small angle neutron scattering technique). The new power law regime will be discussed further below.

In order to validate the present findings we note that according to theory [2,5], the volume fraction of the polymer, $\phi^\dagger$, where the crossover from marginal solvent behavior to θ solvent behavior occurs, is obtained from

$$\phi^\dagger \approx (1-2\chi). \tag{14}$$

Here χ is Flory-Huggins interaction parameter. Thus χ of the solution can be estimated to be ≈ 0.45 from the result $\phi^\dagger \approx 0.1$. This χ value is similar to the interaction parameter ($\chi=0.42$) of the solution of PMMA in toluene, a solution with nearly identical polymer-solvent miscibility [34] as the present system. With decreasing concentration the solution is further predicted [2,5] to exhibit a marginal solvent behavior until $\tilde{\phi}$, where ξ_s reaches the radius of thermal blob, ξ_τ:

$$\tilde{\phi} = \frac{3}{4\pi}\frac{(1-2\chi)}{n^3}. \tag{15}$$

Here the parameter n is proportional to the number of bonds in a Kuhn segment defined by $C_\infty/6$, where C_∞ is the characteristic ratio [5,9]. Using the relation $n=C_\infty/6=1.36$ our system is therefore roughly expected to have a marginal solvent behavior from $\tilde{\phi}=0.01$ to $\phi^\dagger \approx 0.1$. The prediction thus is in nice agreement with the present result.

In the highly concentrated regime, approximately $0.3 < \phi < 0.6$, the polymer fraction dependence theory [2,5] is found not to be applicable. Experimentally a power law exponent $\alpha_3 \approx 2$ is found, while the theory predicts $\alpha_3=0$ when ξ_s is comparable to the persistence length of the polymer [31] (≈ 1 nm). A strong decrease in ξ_s in the highly concentrated regime has also been observed for other polymer solutions [32,33]. This has been attributed to the proximity to the glass transition of the polymer [32]. However, a similar decrease has also been observed in the highly concentrated regime of solutions of PDMS in octane [33]. These experiments were performed at around 300 K, i.e., even well above the T_g of bulk PDMS (~ 146 K). Furthermore, in the present study we observe an exponent $\alpha_3 \approx 2$ also at 400 K as shown in Fig. 5. This suggests that the strong decrease is not due to the glass transition, and instead, we will discuss effects of the local structure at high polymer concentrations.

The unperturbed wormlike chain model proposed by Kratky and Porod [35] shows that sequences of the persistence length scale can be described by rodlike segments. In analogy with the polymer fraction dependence theory we assume that the rodlike segments are perturbed by the contact with other rodlike segments. In this condition, the segments can be only correlated between the contacts, and ξ_h can be recognized as the length of the segment between the contacts as shown in Fig. 6(a). These contacts are expected to be ternary since the two-body interactions have already vanished at the crossover from a marginal to a θ solvent behavior [2,5]. Therefore, if our assumption is appropriate, ξ_h is expected to be proportional to the number of the monomers, g_3, between the ternary contacts. Following a similar treatment as in Refs. [2] and [5], ξ_h can then be expressed as

$$\xi_h \sim g_3 = \frac{\rho_{chain}}{\rho_{ternary}} \sim \frac{\phi}{\phi^3} = \phi^{-2}, \tag{16}$$

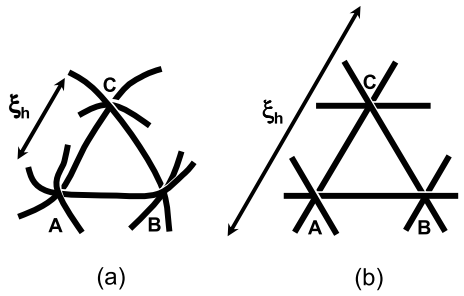

FIG. 6. Qualitative picture of a concentrated polymer solution at persistence length scale: *A*, *B*, and *C* are ternary contacts between different chains. (a) A flexible rodlike segment model: the motions of the monomers are only correlated between the ternary contacts. ξ_h is recognized as a characteristic length between the contacts. (b) A rigid rod segment model: the motions of the monomers are correlated beyond the ternary contacts. ξ_h is recognized as an unperturbed persistence length.

where ρ_{chain} is the number of polymer chains per unit volume and $\rho_{ternary}$ is the number of ternary contacts per unit volume. Indeed, a power law dependence, $\alpha_3=2$, is very close to what is observed in the present study as well as in some previous studies.

The only difference between the conventional model (the polymer fraction dependence theory) and our extended version of the model is the different interpretation of the dynamics of a rodlike segment at the persistence length scale as discussed above and shown in Fig. 6. In the new model, the segment is assumed to be flexible enough so that a longitudinal elastic force such as the osmotic elastic force can screen the motions of the monomers beyond the ternary contacts (a flexible rodlike segment model). On the other hand, in the conventional model the segment is assumed to behave like a complete rigid rod. Thus the motions of the monomers are correlated beyond the ternary contacts without the influence of uncorrelated monomers belonging to the other chains (a rigid rod segment model). Experimentally, the persistence length is observed to decrease when the temperature is elevated [36]. This behavior is in agreement with our experimental observation that ξ_h at 400 K is smaller than at 300 K in the highly concentrated regime (see Fig. 5). Therefore, the present result infers that a complete rigid rod assumption is less appropriate and the conventional model may be oversimplified at the highly concentrated regime. This complete rigid rodlike behavior is expected to be limited to the case that ξ_s approaches the size of the bond length of the monomers. According to literature data [32] of the solution of polystyrene in toluene, ξ_s is found to be independent of the polymer concentration when reaching the bond length of the monomer (0.2 nm).

V. CONCLUSIONS

In the present paper, we have examined the power law crossovers of ξ_h in a polymer solution of poly(methyl methacrylate) in propylene carbonate ranging from the semidilute regime to the highly concentrated regime at 300 and 400 K. Without taking account of η_{local}, we observe unrealistic crossovers of the power laws with increasing ϕ. However, after taking η_{local} into account, sharp crossovers between marginal and θ behavior is observed at both temperatures with increasing ϕ. In the highly concentrated regime where ξ_s is comparable to the persistence length of the polymer, a new power law is observed with an exponent, $\alpha\approx 2$. The observation is supported by literature data reporting on ξ_s. A new model based on flexible rodlike segments at the persistence length scale is proposed in the present study. The model predicts a power law exponent in excellent agreement with the present experimental results.

ACKNOWLEDGMENTS

Financial support from the Swedish Foundation for Strategic Research is gratefully acknowledged. Dr. Patrik Johansson is acknowledged for electron density calculations to determine the volumes of the molecules.

[1] P.G. de Gennes, Macromolecules **9**, 594 (1976).
[2] D.W. Schaefer and C.C. Han, in *Dynamic Light Scattering: Applications of Photon Correlation Spectroscopy*, edited by R. Pecora (Plenum Press, New York, 1985).
[3] W. Brown and T. Nicolai, Colloid Polym. Sci. **268**, 977 (1990).
[4] M. Daoud and G. Jannink, J. Phys. (Paris) **37**, 973 (1976).
[5] D.W. Schaefer, Polymer **25**, 387 (1984).
[6] M. Doi and S.F. Edwards, *The Theory of Polymer Dynamics* (Clarendon Press, Oxford, 1986).
[7] B. Farnoux, F. Boué, J.P. Cotton, M. Daoud, G. Jannink, M. Nierlich, and P.G. de Gennes, J. Phys. (Paris) **39**, 77 (1978).
[8] T. Norisuke and H. Fujita, Polym. J. (Tokyo, Jpn.) **14**, 143 (1982).
[9] L.H. Sperling, *Introduction to Physical Polymer Science* (Wiley-Interscience, New York, 2001), pp. 165–200.
[10] W. Brown and P. Stepanek, Macromolecules **24**, 5486 (1991).
[11] W. Brown, R.M. Johnsen, C. Konak, and L. Dvoranek, J. Chem. Phys. **95**, 8568 (1991).
[12] W. Brown and T. Nicolai, Nuovo Cimento Soc. Ital. Phys., D **16D**, 661 (1994).
[13] T. Koch, G. Strobl, and B. Stühn, Macromolecules **25**, 6255 (1992).
[14] R.A. Waggoner, F.D. Blum, and J.M.D. MacElroy, Macromolecules **26**, 6841 (1993).
[15] L. Masaro and X.X. Zhu, Prog. Polym. Sci. **24**, 731 (1999).
[16] J.S. Vrentas, J.L. Duda, H.-C. Ling, and A.-C. Hou, J. Polym. Sci., Polym. Phys. Ed. **23**, 289 (1985).
[17] O.F. Bezrukov, V.P. Budtov, B.A. Nikolayev, and V.P. Fokanov, Polym. Sci. U.S.S.R. **13**, 988 (1971).
[18] T. Nicolai and W. Brown, Macromolecules **29**, 1698 (1996).
[19] TITAN v1.0 (copyright © 1999, Wavefunction Inc. Schrödinger Inc.) The calculations were performed using the default cutoff electron density of 0.002 $e/\text{Å}^3$.
[20] C. Svanberg, J. Adebahr, H. Ericson, L. Börjesson, L.M. Torell, and B. Scrosati, J. Chem. Phys. **111**, 11 216 (1999).
[21] C.H. Wang, Prog. Colloid Polym. Sci. **91**, 138 (1993).

[22] A. Faraone, S. Magazù, G. Maisano, R. Ponterio, and V. Villari, Macromolecules **32**, 1128 (1999).
[23] M. Heckmeier, M. Mix, and G. Strobl, Macromolecules **30**, 4454 (1997).
[24] E. Geissler and A.M. Hecht, J. Phys. (Paris), Lett. **40**, L173 (1979).
[25] S. Magazù, V. Villari, A. Faraone, G. Maisano, and S. Jonssen, J. Chem. Phys. **116**, 427 (2002).
[26] A. Bondeau and J. Huck, J. Phys. (Paris) **46**, 1717 (1985).
[27] D. Andersson, C. Svanberg, J. Swenson, W.S. Howells, and L. Börjesson, Physica B **301**, 44 (2001).
[28] J. Huck, A. Bondeau, G. Noyel, and L. Jorat, IEEE Trans. Electr. Insul. **23**, 615 (1988).
[29] U. Schneider, P. Lunkenheimer, R. Brand, and A. Loidl, Phys. Rev. E **59**, 6924 (1999).
[30] C. Svanberg, W. Pyckhout-Hintzen, and L. Börjesson (unpublished): ξ_s data for the solutions of PMMA ($M_w = 1\,587\,000$) with PC.
[31] M. Tricot, Macromolecules **19**, 1268 (1986).
[32] W. Brown, K. Mortensen, and G. Floudas, Macromolecules **25**, 6904 (1992).
[33] F. Horkay, A.-M. Hecht, H.B. Stanley, and E. Geissler, Eur. Polym. J. **30**, 215 (1994).
[34] E.A. Grulke, in *Polymer Handbook*, edited by J. Brandrup, E. H. Immergut, E.A. Grulke, A. Abe, and D.R. Bloch (Wiley-Interscience, New York, 1999), Chap. VII, p. 675.
[35] O. Kratky and G. Porod, Recl. Trav. Chim. Pays-Bas **68**, 1106 (1949).
[36] K. Teruo, Y. Terao, A. Teramoto, N. Nakamura, M. Fujiki, and T. Sato, Macromolecules **34**, 4519 (2001).